ADVANCED HEALTHCARE MATERIALS
www.advhealthmat.de

Magnetothermal Miniature Reactors Based on Fe_3O_4 Nanocube-Coated Liquid Marbles

*Hualin Li, Peng Liu, Renardi Gunawan, Zemenu Mengistie Simeneh, Chen Liang, Xi Yao, and Mengsu Yang**

Liquid marbles have recently attracted much interest in various scientific fields because of their isolated environment and robustness. However, conventional liquid marbles lack a reliable heating mechanism, which is critical in many potential applications. Here, the development of iron oxide (Fe_3O_4) nanocube-coated liquid marbles (iNLMs), which can be homogeneously heated with an alternating magnetic field (AMF) to as high as 86 °C, is reported. Through tuning the power of the AMF, the iNLMs canbe heated to desired temperatures in controllable patterns. Furthermore, multicenter and selective heating is realized based on the unique magnetothermal properties of iNLMs. As heatable miniature reactors, the iNLMs are further demonstrated to facilitate the kinetic study of temperature-dependent chemical reactions. DNA amplification is successfully performed in liquid marbles, achieving a 25% superior amplification rate compared with that in a common thermal cycler. These results confirm the feasibility of coating liquid marbles with Fe_3O_4 nanocubes to form delicate magnetothermal miniature reactors, which provides a reliable method of applying liquid marbles in areas such as biosensor technology, point-of-care testing, and theranostics.

In recent years, liquid marbles as miniature reactors have been a fast-developing concept[1] owing to their ability to contain liquid in microliter quantities, simplicity in fabrication and manipulation, and excellent mechanical robustness. Based on these properties, liquid marbles have been applied in chemical reactions,[2] surface-enhanced Raman spectroscopy (SERS)/electrochemical platform,[3] 3D cell culture,[4] and drug sensitivity tests for chemotherapy[5] and phototherapy.[6] However, because of the lack of a proper heating mechanism, current applications of liquid marbles are restricted to reactions with low activation energy requirements or at room temperature. Previously a heating mechanism for liquid marbles was reported based on laser irradiation.[7] This heating mechanism has several limitations: direct contact was required between liquid marbles and laser beams; only the laser-activated part of liquid marbles were heated; the position of the liquid marbles was strictly restricted due to fixed position of the laser generator; and only one liquid marble could be heated under one laser generator. These limitations inhibit the large-scale application of liquid marbles in industry and biomedical sciences.

A series of magnetically-actuated liquid marbles have been fabricated for sample storage, controlled manipulation, and "online" detection.[2,8] However, all previous magnetic-field-responsive liquid marbles have been applied under stationary magnetic fields, and the functions of magnetic particles on liquid marbles are limited to force mediator and coating phase. Magnetic hyperthermia, which is noninvasive, remotely operatable, and highly selective, is developing rapidly for magnetothermal cancer therapy and controlled drug release.[2,8] Crucially, magnetic hyperthermia requires incorporation of an alternating magnetic field (AMF) rather than a stationary magnetic field. Therefore, the development of magnetic liquid marbles as heatable miniature bioreactors with AMF is promising but challenging. Iron oxide (Fe_3O_4) nanoparticles are thus far the most widely accepted nanostructures as biocompatible heat mediators in magnetic hyperthermia, signified by their abundance in both preclinical and clinical research.[9] They have relatively high saturation magnetization and low residual magnetization, and are easy to be surface-functionalized for different purposes.

Herein, we report the fabrication of Fe_3O_4 nanocube-coated liquid marbles (iNLMs) and their application as AMF-triggered heatable miniature reactors for reaction kinetics study and DNA amplification. We characterized the magnetic actuation and mechanical properties of iNLMs as controllable and robust miniature reactors. Furthermore, we evaluated the remote, multicenter, or repeated heating of iNLMs with peak bulk temperature from 27 °C to 86 °C by controlling the AMF power (5–30 mT with fixed frequency of 350 kHz). The application of iNLMs for

Dr. H. Li, Dr. P. Liu, R. Gunawan, Z. M. Simeneh, C. Liang, Dr. X. Yao, Prof. M. Yang
Department of Biomedical Sciences
City University of Hong Kong
83 Tat Chee Ave, Kowloon Tong, Hong Kong SAR, P. R. China
E-mail: bhmyang@cityu.edu.hk

Dr. H. Li, Dr. P. Liu, R. Gunawan, Z. M. Simeneh, C. Liang, Dr. X. Yao, Prof. M. Yang
Key Laboratory of Biochip Technology
Biotechnology and Health Centre
City University of Hong Kong Shenzhen Research Institute
Shenzhen 518057, P. R. China

The ORCID identification number(s) for the author(s) of this article can be found under https://doi.org/10.1002/adhm.202001658

DOI: 10.1002/adhm.202001658

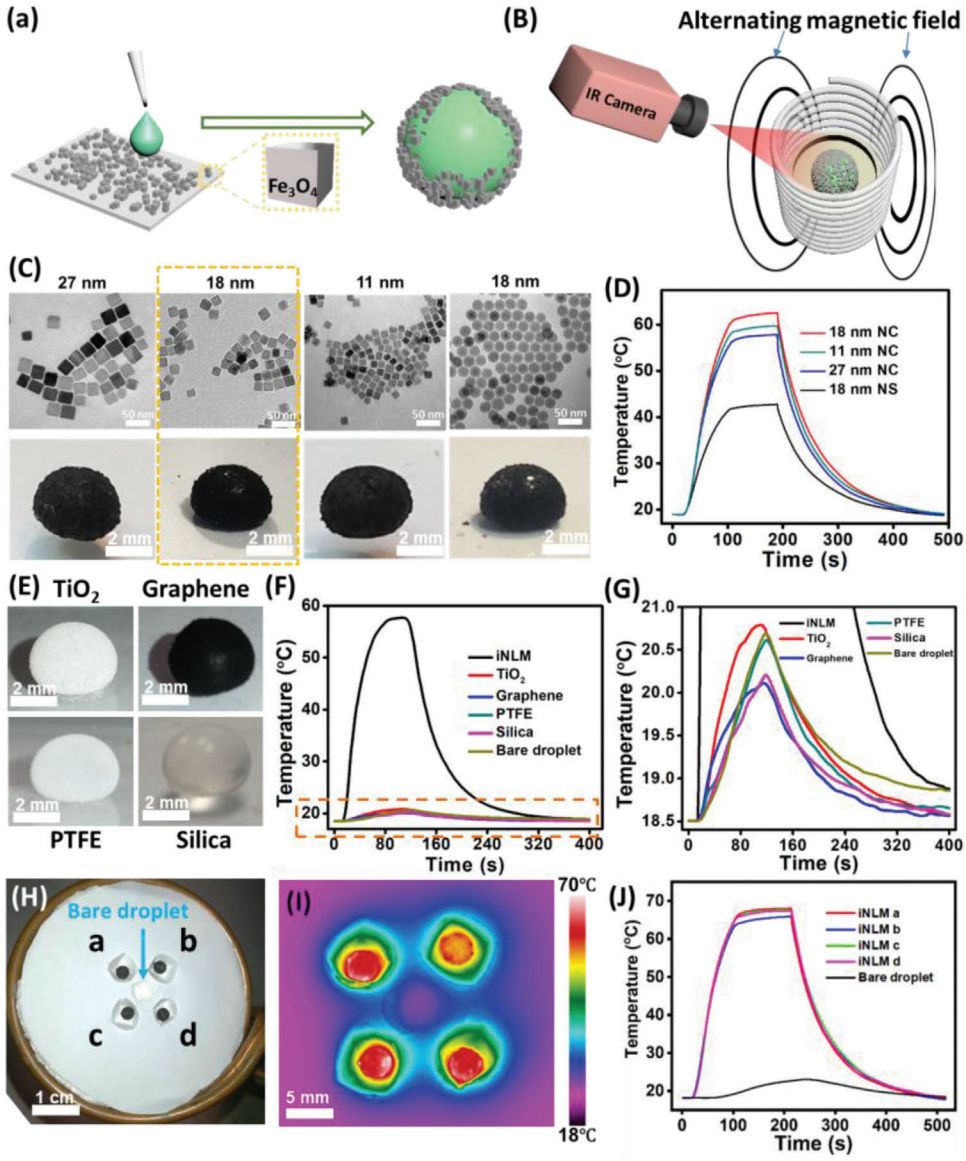

Figure 1. A) Preparation of Fe_3O_4 nanocubes-coated liquid marbles (iNLMs). B) Schematic representation of the AMF setup and temperature detection. C) TEM/digital images of 40 µL liquid marbles coated by different types of Fe_3O_4 nanoparticles. D) Bulk temperature–time profiles of four different liquid marbles under 20 mT and 350 kHz in (C). E) Digital images of liquid marbles coated by other materials. F) Bulk temperature–time profiles of liquid marbles coated by different materials. G) Zoom-in of a selected part in (F) to show the slight temperature change of liquid marbles coated by materials other than Fe_3O_4 nanocubes. H) Setup of multicentric heating in the AMF. I) Thermograms indicate the temperature of iNLMs and water droplets in a plateau state. J) Bulk temperature–time profiles of iNLMs and water droplets during the heating and cooling process.

reaction kinetics modulation was subsequently realized by performing temperature-dependent degradation of methylene blue. DNA amplification was carried out in liquid marbles with homogeneous heating induced by exposure to an AMF.

In this study, iNLMs were fabricated by rolling microliter water droplets on a bed of hydrophobic Fe_3O_4 nanocubes (**Figure 1**A). Fe_3O_4 nanocubes are highly hydrophobic, and their well-defined edges/tips can generate unprecedented localized magnetic heating.[10] They were synthesized by well-developed thermal decomposition methods using oleic acid as the surfactant.[11] According to a previously reported procedure,[11] different heating rates were chosen to synthesize Fe_3O_4 nanocubes of different sizes with a highly crystalline phase and hydrophobicity. The magnetic thermal behavior of iNLMs was investigated upon AMF exposure, and its spatial temperature profiles were recorded using an infrared (IR) camera (Figure 1B). Three different sizes (27.3 ± 2.8, 18.4 ± 2.5, and 10.8 ± 1.9 nm) of Fe_3O_4 nanocubes and 18.1 ± 3.5 nm of Fe_3O_4 nanosphere were synthesized and charaterized by transmission electron microscopy images (Figure 1C,D). Bulk temperature curves revealed that the 18.4 nm iNLMs exhibited the highest magnetothermal temperature and efficiency during the same heating process among the four sizes and shapes. To further determine the magnetic properties of these four types of Fe_3O_4 nanoparticles,

magnetic measurements were conducted for each sample. The results revealed that the Fe_3O_4 nanocubes exhibited typical superparamagnetic behaviors (Figure S1A, Supporting Information), and the 18.4 nm Fe_3O_4 nanocubes achieved higher saturation during a shorter field exposure time. Additionally, as different nanoparticle anisotropy would contribute to different heating capability,[12] this may explain why the 18.4 nm iNLMs showed the highest magnetothermal efficiency under AMF. Accordingly, the 18.4 nm iNLMs were selected for subsequent experiments.

The synthesized 18.4 nm Fe_3O_4 nanocubes were further characterized with X-ray powder diffraction (XRD) (Figure S1B, Supporting Information). The particle size was measured as 15.8 nm based on calculation using Scherrer equation from the reflection peak of (311) in the XRD pattern. The measurement is close to the 18.4 ± 2.5 nm particle size based on the TEM image calculation.[13] The sizes of iNLMs can be tuned by changing the volume of water droplets between 5 and 300 µL (Figure S2, Supporting Information), indicating the versatility of these miniature reactors in terms of reaction capacity. Furthermore, iNLMs exhibited high contact angles of approximately 145°. Under 23°C and 60% humidity, water evaporation from 40 µL iNLMs and 40 µL bare droplets placed on the surface of a Petri dish were measured by relative weight change at different time points, revealing that iNLMs had a 38.8% longer survival time compared with bare droplets (Figure S3, Supporting Information). Through these evaporation experiments, we estimated that the mass of Fe_3O_4 coated on each 40 µL iNLM was 1.05 ± 0.02 mg. To evaluate the layers of Fe_3O_4 nanocubes on each 40 µL iNLM, the surface area of the iNLMs is approximately equal to a sphere with a volume of 40 µL, which would be 1063.62 nm^3. Considering that the density of Fe_3O_4 is 5.17 g cm^{-3} and the average volume of a 18.4 nm Fe_3O_4 nanocube is 6229.5 nm^3, there are approximately 195 layers of Fe_3O_4 nanocubes on each 40 µL iNLM, which means the thickness of the Fe_3O_4 nanocube coating on the liquid marbles was approximately 3.59 µm. The formed iNLMs were easy to handle and could be reversibly opened and closed, or be controlled to move in different directions under the actuation of a magnet owing to their magnetic nature and robustness (Figure S4A,B, Supporting Information). With a magnet and a pipette, liquid could be added into or withdrawn from the iNLMs, which offers the potential for carrying out multistep solution reaction (Figure S4C, Supporting Information).

Our iNLMs possessed unique magnetothermal heating properties over liquid marbles coated with other materials. Only few elements such as iron, nickel, and cobalt and their alloys would respond to magnetic fields; therefore, we tested five types of liquid marbles coated by different materials: Fe_3O_4 nanocubes, titanium oxide, graphene, polytetrafluoroethylene (PTFE), and silica nanoparticles, and bare droplets without any coating were set as control (Figure 1E). Upon AMF exposure (20.0 mT), the iNLMs exhibited the highest bulk temperature of approximately 58 °C (Figure 1F), which is ≥2.8 times higher than liquid marbles of other materials (≤20.8 °C). Furthermore, the temperature change (ΔT = 40 °C) of the iNLMs was ≥18-fold higher than that of other liquid marbles (ΔT ≤2.2 °C) (Figure 1G). The slight temperature increase of the bare droplets and liquid marbles coated by other materials are probably caused by heat radiation from the copper coils, which were mildly heated when the AMF was generated.

Thus far, it has been challenging to exert heating of multiple liquid marbles simultaneously,[7a] which restricts liquid marbles from being used for series studies. As the AMF covered a large area, which was illustrated through the simulation in COMSOL (Figure S5, Supporting Information), the iNLMs located in the AMF could be simultaneously heated, indicating that parallel heating of multiple iNLMs is possible. Here, four liquid marbles and one bare droplet were placed under the same AMF (Figure 1H). In the initial state, an IR image suggested that all five targets shared similar temperature of 18.5 °C (Figure S6A, Supporting Information). When the AMF was triggered, the four liquid marbles were heated immediately, and the bare droplet remained at room temperature (Figure 1I; Video S1, Supporting Information). After AMF exposure for 90 s, all four liquid marbles were homogeneously heated to reach the highest bulk temperature of approximately 60 °C, while the bare droplet remained at room temperature (approximately 20 °C) (Figure 1J; Figure S6B, Supporting Information).

The bulk temperature and temperature distribution of iNLMs were investigated upon AMF exposure, and their spatial temperature profiles upon different powers of AMF were monitored using an IR camera. During the heating process, a 40 µL iNLM exhibited a homogeneous surface temperature of 18.5 °C prior to AMF exposure (**Figure 2**A, 0 s). Within 5/10/20/40/80 s of AMF (20 mT) exposure, the average temperature of the whole iNLM increased to approximately 26.6/32.3/40.5/49.8/61.5°C (Figure 2C), with a temperature change rate $(dT/dt)_{max}$ of 4.63°Cs^{-1} (Figure S7A, Supporting Information). Due to the fact that Fe_3O_4 nanocubes were uniformly distributed on the whole surface of liquid marbles, AFM activation enabled 360° heating such that the temperature distribution of iNLMs during the whole heating process was homogenous, which is a dramatic improvement compared with a previous laser-induced heating system.[7a] Once the AMF was switched off, the iNLMs entered a cooling process. Similarly, the temperature distribution during the cooling process was also homogenous (Figure 2B). The longer cooling process to room temperature was due to slower heat dissipation from the iNLMs to air. Overall, the results highlighted the rapid and homogenous magnetothermal properties of iNLMs and their heat conductivity for achieving immediate thermal modulation.

The temperature of our iNLMs can be precisely modulated by AMF power. Equilibrium temperature (at t = 90 s) from 26 °C to 87 °C was achieved by tuning the AMF power from 5.0 to 30.0 mT, respectively (Figure 1E). Under different AMF powers, the maximum temperature increase rate (dT/dt) during the heating process, which was indicated by the 1st derivative of temperature change, ranged from 0.31 °C to 4.63 °C s^{-1} (Figure S7A, Supporting Information). In general, the magnetic thermal behavior of iNLMs can be categorized as a three-step heating process. First, the drastic temperature increase in the first 10 s (10 to 20 s) was attributed to the instantaneous magnetic thermal transduction of Fe_3O_4 under AMF treatment. Then, the surface layer of encapsulated water was initially heated by heat generated in the whole shell of the iNLMs and conducted to water in all directions, while the internal part of the encapsulated water remained at a low temperature. The dramatic temperature difference between the surface and internal part of the encapsulated water triggered intense convection within the iNLMs, which led to a slow but continuous

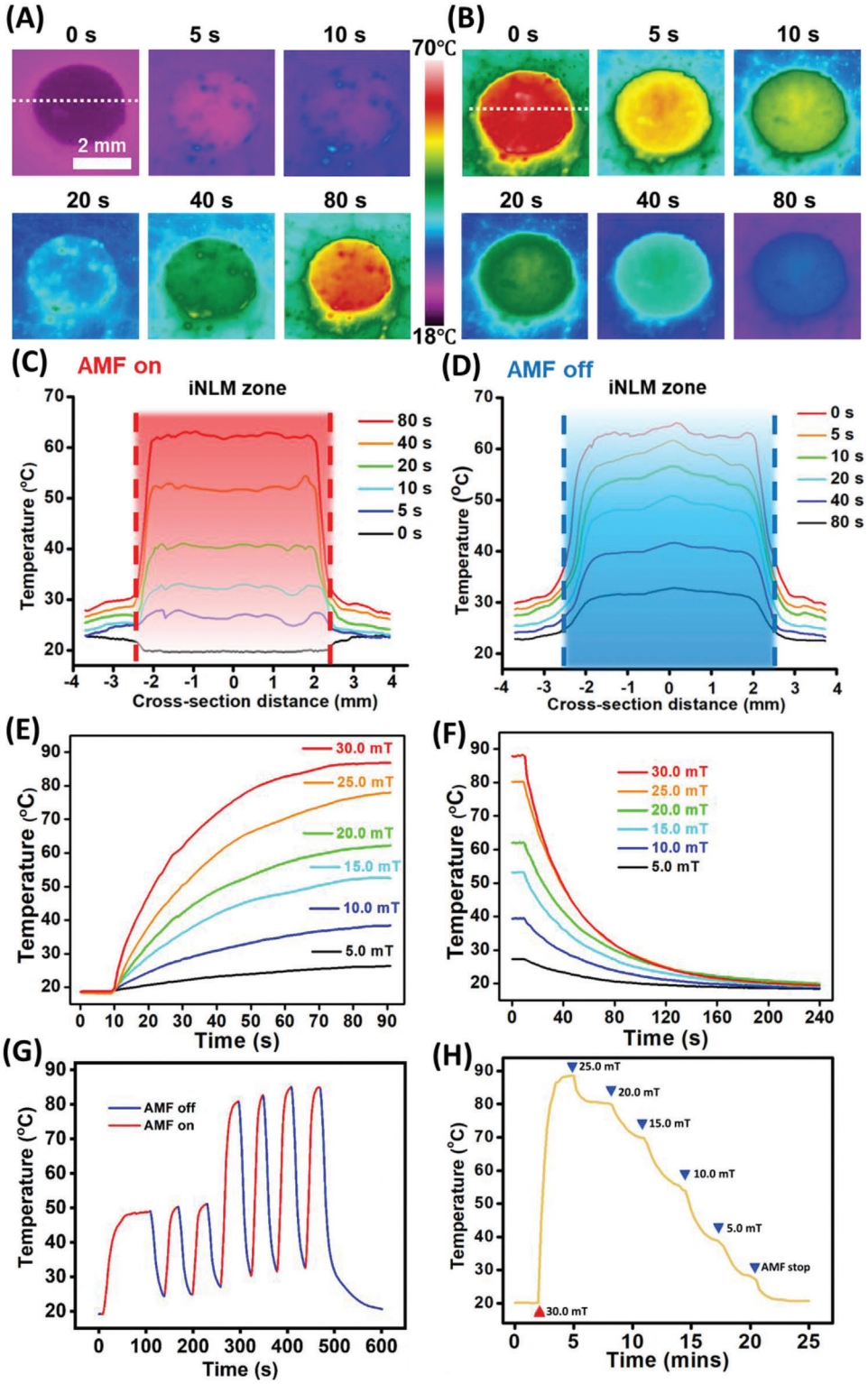

Figure 2. A,B) Thermograms of a 40 µL iNLM under exposure to 20 mT AMF. Spatial temperature profiles on the iNLM along the white dotted line when the AMF generator was C) switched on and D) off, respectively. Temperature-time profiles of E) the heating process under exposure to different powers of AMF and F) the cooling process when the AMF generator was switched off. G) Temperature–time profiles of heating/cooling cycles on the iNLM. H) Temperature–time profiles of controlled step cooling process.

temperature increase from 20 to 80 s. Lastly, when the convection in the encapsulated water had almost finished, a subsequent temperature plateau appeared (after 80 s, Figure 2E). The plateau indicates that thermal equilibrium has been reached, in which the gain of heat energy through the magnetic field is balanced by heat dissipation through thermal conduction on the surface of the iNLM shell, the encapsulated water, and the environment (including the surrounding air and the holding surface).

Next, the cooling process of the iNLM was studied by switching off the AMF generator. Similar to the heating process, the cooling process of the whole iNLM also occurred in three stages (Figure 2F; Figure S7B, Supporting Information). First, temperature under different AMF dropped substantially in the first 10 s (10 to 20 s). Then, inner convection might be triggered, and a gradual temperature decrease of the entire iNLM continued for approximately 200 s before eventually reaching a plateau, which is 2.5 times longer than the heating process. The longer duration may be due to the slow dissipation from the iNLMs to air as the main mechanism of heat transfer in cooling, whereas direct conduction - which is known to be more effective than dissipation - from Fe_3O_4 to water is the main mechanism of heat transfer in heating.[14]

The rapid responsiveness and high reproducibility of magnetothermal heating were further examined by subjecting a 40 µL iNLM to controlled cycling or step cooling in AMF with different powers. In controlled temperature cycles, the iNLM was heated to approximately 50 °C under a 15.0 mT AMF followed by two 1-min cycles, and then the power was increased to 30.0 mT and the equilibrium temperature was increased to approximately 80 °C for another four cycles (Figure 2G; Figure S8A, Supporting Information). In the controlled cooling experiments, the iNLM was heated with a 30.0 mT AMF during the 2nd to 5th min (Figure 2H). Then, the AMF power was reduced to 25.0 mT at the 5th min, and 3 min later, the AMF power was further reduced to 20.0 mT, and so on until the AMF was turned off (Figure 2H; Figure S8B, Supporting Information). The steady temperature change and control through adjusting the AMF indicated that the iNLM could be utilized in a process that required complicated temperature control. Hence, the iNLM demonstrated timely and precise thermal control by AMF, which is essential for reactions with delicate temperature requirements.

Next, iNLMs as remotely heatable miniature reactors were evaluated by analyzing the degradation of temperature-dependent methylene blue (**Figure 3**A,B). Methylene blue would be reduced to a colorless product by $NaBH_4$ in solution upon heating. However, this reduction reaction was nearly inactivated at room temperature. Without $NaBH_4$ addition, less than 2% of methylene blue degradation was observed even after 10 min of exposure to a 15 mT AMF (Figure S9, Supporting Information). Higher temperatures would further enhance this reduction and longer times would lead to more degradation, making it an ideal reaction for tracing temperature change in solution. Typically, 40 µL iNLMs, containing 0.9 mM methylene blue and 0.5 M $NaBH_4$, were exposed to AMF (power = 0, 5, 10, and 15 mT). As a control, bare droplets containing the same component and placed on a layer of Fe_3O_4 nanocubes were used as the control. At predefined time intervals (30 s in the first 4 min and then 2 min in the next 6 min), the encapsulated aqueous solutions or solutions in bare droplets were extracted and measured using UV-Visible spectroscopic measurement (Nanodrop 2000). Thermograms illustrated that 360° irradiation and heating enabled the iNLMs to reach a much higher temperature than droplets on a coating layer, in which only the bottom solution is heated (Figure 3C,D). From the obtained absorbance spectra of methylene blue in iNLMs, a significant decrease of the characteristic 608 nm peak intensity was observed, indicating its degradation during AMF exposure (Figure 3E; Figure S10, Supporting Information). Consequently, a degradation efficiency of >98% was achieved in a 15 mT AMF, as shown by $C_{10min}/C_0 = 0.02$ (C_0 and C_{10min} denote the initial concentration and concentration after 10 min of AMF exposure, Figure 3F; Figure S11, Supporting Information). Without any heating (room temperature = 19 °C), the degradation efficiency of MB after 10 min was 18.8%. The degradation efficiency of MB could reach 60.0%, 75.3%, or 96.7% after 10 min treatments of 5, 10, or 15 mT AMF, respectively (Figure 3F). Because [$NaBH_4$] = 0.5 M >> [Methylene Blue] = 0.9 mM, this reaction was assumed to be a pseudo-first-order reaction: $\ln([MB]/[MB]_0) = -kt$ (k means the degradation rate constant of methylene blue and t means the degradation time). Without any heating (AMF power = 0 mT), k was calculated as 0.020. Through the fitting curve above, k was calculated as 0.088, 0.185, and 0.344 min^{-1} for AMF powers of 5, 10, and 15 mT, respectively (Figure 3G). In the control group, because only the bottom of the mixture in droplets were heated up by the surface coating (Figure 3D), the degradation efficiency and rate were much lower than iNLMs under the same AMF (15 mT), namely only 68.3% and 0.112 min^{-1}, respectively (Figure 3H). The 360° irradiation and heating properties of iNLMs stimulated degradation efficiency from 68.3% in the control group to 96.7% and achieved a 3.1-fold superior reaction rate constant compared with the simple coating layer.

Liquid marbles have recently been applied for high-throughput drug screening,[5] photodynamic therapy,[15] and 3D cell culture.[4a,b,d,16] However, previous reactors based on liquid marbles were unable to carry out heat-triggered molecular biological reactions. To demonstrate the versitility of the iNLMs developed in this study, we performed the DNA amplification reaction in liquid marbles for the first time, by using the loop-mediated isothermal amplification (LAMP) assay. Typically, 40 µL iNLMs containing LAMP master mixture, the target human papillomavirus (HPV) DNA, and primers were exposed to AMF and reached specific working temperature (65 °C) (**Figure 4**A). To prevent undesirable evaporation of iNLMs during long incubation periods, the 40 µL iNLMs were stored in Eppendorf tubes and placed in an AMF (Figure 4B). Because of the multicentric heating ability of the AMF system, we could test several samples simultaneously (Figure S12A,B, Supporting Information). After tens of minutes of incubation, some negligible evaporation appeared inside the tubes (Figure S12E, Supporting Information), and the tubes were centrifuged to separate the liquid and iron oxide nanocubes (Figure S12E, Supporting Information). The residual transparent liquid was further tested.

In addition to DNA amplification in iNLMs, control experiments were also conducted, in which Eppendorf tubes containing the same components, including a solution mixture of LAMP master mixture, the target HPV DNA, and primers, were incubated in similar temperatures in a thermal cycler. Three

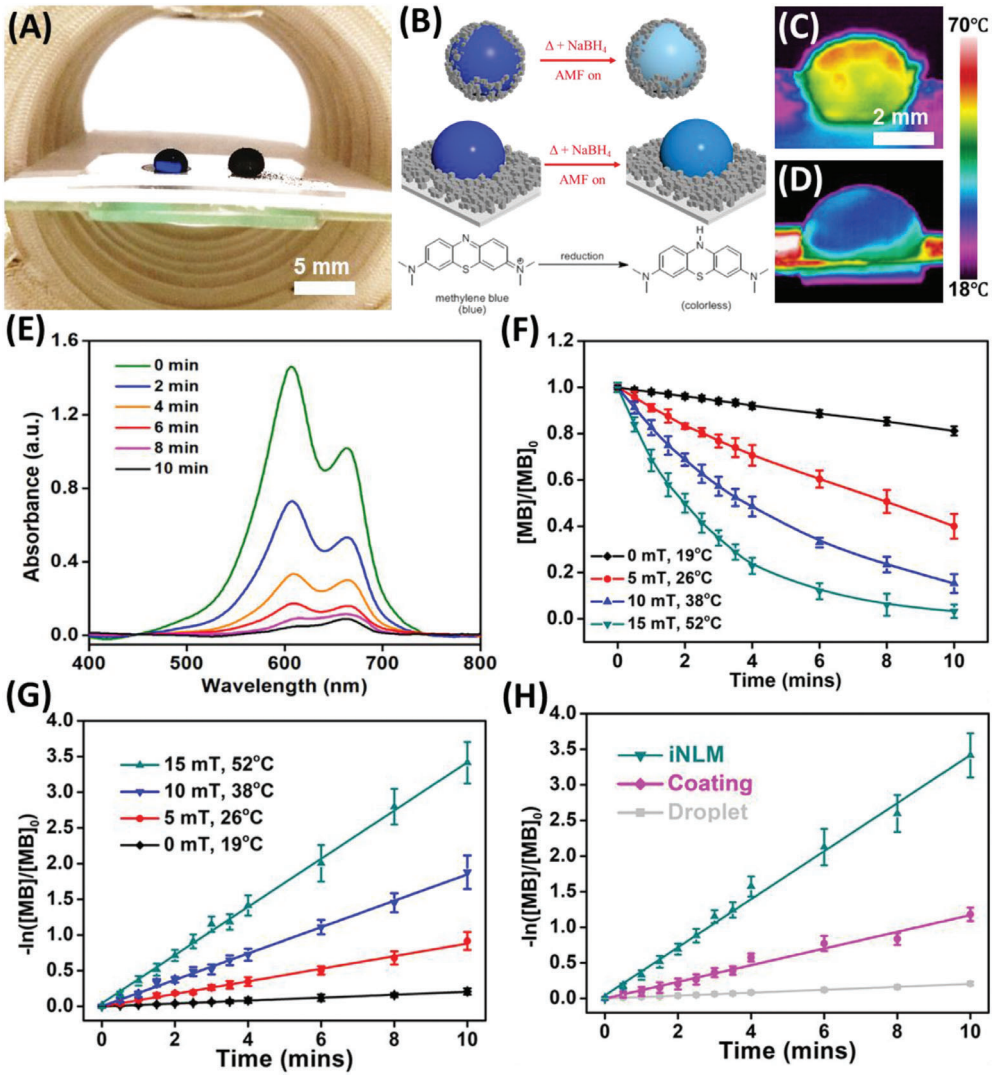

Figure 3. A) Setup and B) schematic representation of an iNLM as a remotely magnetothermal miniature reactor. Thermogram of C) an iNLM and D) a droplet on coating. E) Absorbance spectra of methylene blue solution extracted from iNLMs at different time intervals (AMF power = 15 mT). F) Plot of normalized methylene blue concentrations ($[MB]/[MB]_0$) as a function of irradiation duration for different applied AMF powers. G) Plot of $-\ln([MB]/[MB]_0)$ against irradiation duration for different AMF powers and H) different types of groups according to the pseudo-first-order reaction.

different concentrations of HPV DNA templates, namely 1000, 100, and 10 copies per µL, were tested in the iNLMs and the thermal cycler separately. Considering that the signals of LAMP products were too strong in 1000 copies per µL and too weak in 10 copies per µL, the 100 copies per µL concentration was selected to further illustrate the advantages of iNLMs (Figure S13, Supporting Information). Then, a series of experiments was performed in iNLMs or using thermal cycler with the LAMP reaction time (under 65 °C) ranging from 10 to 60 min. Three methods were used to quantify the amplification results from iNLMs or thermal cycler. First, phenol red staining indicated that the DNA amplification efficiency was higher in iNLMs than in thermal cycler at the same time (Figure 4C,D). In this colorimetric LAMP kit, if DNA amplification occurred, the pH of the mixture would decrease and the phenol red would change from red to yellow. The corresponding absorbance spectra of LAMP products from iNLMs or thermal cycler were used to quantify the color change (Figure 4E,F). A more significant increase in the peak at 436 nm and a more significant decrease in the peak at 588 nm indicated the color change was more obvious in LAMP from iNLMs than that from thermal cycler. Second, calcein was added to another series of products from iNLMs or thermal cycler, and the fluorescence results revealed that the LAMP reaction in iNLMs reached a plateau 10 min earlier than in the thermal cycler (Figure 4H–J), which indicated that the DNA amplification rate in iNLMs was 25% faster than that in thermal cycler. Third, the gel electrophoresis results confirmed that LAMP reactions in iNLMs finished in 40 min, whereas those in thermal cycler required 50 min (Figure 4K). The results further confirmed that because of the larger contact area between the Fe_3O_4 nanocubes and the encapsulated

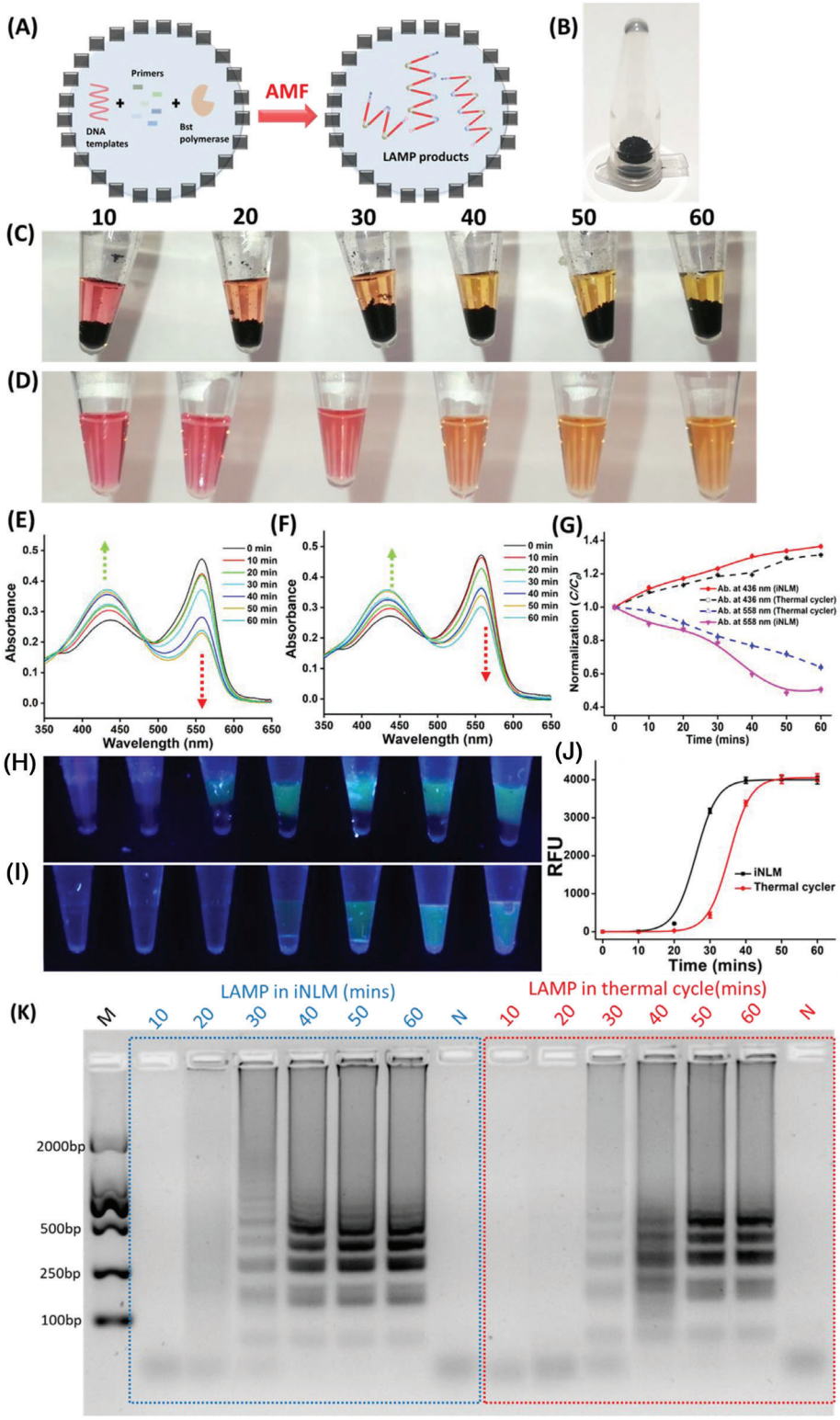

Figure 4. A) Schematic representation of iNLM carrying LAMP assay. B) Digital images of a 40 µL iNLM kept in an Eppendorf tube. LAMP products after different incubation durations (from left to right: 10, 20, 30, 40, 50, and 60 min) from C) iNLM and D) thermal cycler were detected using colorimetric dye (Phenol red). Absorbance spectra of LAMP products after different incubation durations from E) iNLM and F) thermal cycler. G) Plot of peak absorbance of LAMP products from iNLM and thermal cycler against incubation time. Fluorescent images of LAMP products after different incubation durations (from left to right: 0, 10, 20, 30, 40, 50, and 60 min) from H) iNLM and I) thermal cycler. J) Fluorescence intensity against incubation time of LAMP products from iNLM and thermal cycler. K) Agarose gel electrophoresis results of LAMP products. M: Size marker. N: 60-min incubation without HPV DNA template.

solution as well as the spherical geometry to enabling 360° irradiation by AMF, DNA amplification based on a LAMP assay in iNLMs would be faster than that in thermal cycler. Similar results would be expected for other temperature-dependent reactions such as polymerase chain reaction (PCR).

In summary, we described the fabrication of novel iNLMs and their application as magnetothermal bioreactors for reaction kinetics modulation and DNA amplification. This research highlights that through utilizing AMF, controllable, contactless, and multicentric heating of iNLMs could be realized. Homogeneous temperature distribution was observed in iNLMs during heating and cooling. By simply adjusting the power of AMF, iNLMs could be heated to required temperatures from 25 °C to 86 °C, and achieve a 3.1-fold superior reaction rate constant compared with a simple coating layer for the same enzymatic reaction. Notably, through using the LAMP assay, DNA amplification was successfully performed in liquid marbles. This is the first application of liquid marbles in molecular biological reaction. The multiple advantages of iNLMs will enable their further applications in research and industry, including in lab-on-a-chip systems, point-of-care testing, and theranostics.

Supporting Information

Supporting Information is available from the Wiley Online Library or from the author.

Acknowledgements

This work was supported by grants from the General Research Fund (CityU_11303815) and the Research Impact Fund (R1020-18F) of the Hong Kong Research Grant Council, the Guangdong Frontier and Key Technology Development Fund (2017B020226001), and the Shenzhen Knowledge Innovation Program (JCYJ20150601102053070), P. R. China.

Conflict of Interest

The authors declare no conflict of interest.

Keywords

DNA amplification, liquid marbles, magnetothermal reactors, miniature bioreactors, nanoparticles

Received: September 17, 2020
Revised: November 17, 2020
Published online: January 20, 2021

[1] a) P. Aussillous, D. Quere, *Nature* **2001**, *411*, 924; b) N. M. Oliveira, R. L. Reis, J. F. Mano, *Adv. Healthcare Mater.* **2017**, *6*, 1700192; c) E. Bormashenko, *Langmuir* **2017**, *33*, 663; d) S. Fujii, S.-i. Yusa, Y. Nakamura, *Adv. Funct. Mater.* **2016**, *26*, 7206.

[2] a) Y. Xue, H. Wang, Y. Zhao, L. Dai, L. Feng, X. Wang, T. Lin, *Adv. Mater.* **2010**, *22*, 4814; b) Y. Zhao, J. Fang, H. Wang, X. Wang, T. Lin, *Adv. Mater.* **2010**, *22*, 707; c) Y. Zhao, Z. Xu, H. Niu, X. Wang, T. Lin, *Adv. Funct. Mater.* **2015**, *25*, 437; d) Z. Liu, T. Yang, Y. Huang, Y. Liu, L. Chen, L. Deng, H. C. Shum, T. Kong, *Adv. Funct. Mater.* **2019**, *29*, 1901101.

[3] a) H. K. Lee, Y. H. Lee, I. Y. Phang, J. Wei, Y.-E. Miao, T. Liu, X. Y. Ling, *Angew. Chem.* **2014**, *126*, 5154; b) C. S. L. Koh, H. K. Lee, G. C. Phan-Quang, X. Han, M. R. Lee, Z. Yang, X. Y. Ling, *Angew. Chem., Int. Ed.* **2017**, *56*, 8813.

[4] a) T. Arbatan, A. Al-Abboodi, F. Sarvi, P. P. Chan, W. Shen, *Adv. Healthcare Mater.* **2012**, *1*, 467; b) R. K. Vadivelu, C. H. Ooi, R. Q. Yao, J. T. Velasquez, E. Pastrana, J. Diaz-Nido, F. Lim, J. A. Ekberg, N. T. Nguyen, J. A. St John, *Sci. Rep.* **2015**, *5*, 15083; c) K. Lin, R. Chen, L. Zhang, D. Zang, X. Geng, W. Shen, *ACS Appl. Mater. Interfaces* **2019**, *11*, 8789; d) H. Li, P. Liu, G. Kaur, X. Yao, M. Yang, *Adv. Healthcare Mater.* **2017**, *6*, 1700185; e) B. Wang, K. F. Chan, F. Ji, Q. Wang, P. W. Y. Chiu, Z. Guo, L. Zhang, *Adv. Sci.* **2019**, *6*, 1802033.

[5] N. M. Oliveira, C. R. Correia, R. L. Reis, J. F. Mano, *Adv. Healthcare Mater.* **2015**, *4*, 264.

[6] D. Wang, L. Zhu, J. F. Chen, L. Dai, *Angew. Chem.* **2016**, *128*, 10953.

[7] a) W. Gao, H. K. Lee, J. Hobley, T. Liu, I. Y. Phang, X. Y. Ling, *Angew. Chem., Int. Ed.* **2015**, *54*, 3993; b) Y. Chu, F. Liu, L. Qin, Q. Pan, *ACS Appl. Mater. Interfaces* **2016**, *8*, 1273.

[8] Y. Zhao, Z. Xu, M. Parhizkar, J. Fang, X. Wang, T. Lin, *Microfluid. Nanofluid.* **2012**, *13*, 555.

[9] a) J. Mosayebi, M. Kiyasatfar, S. Laurent, *Adv. Healthcare Mater.* **2017**, *6*, 1700306; b) V. F. Cardoso, A. Francesko, C. Ribeiro, M. Banobre-Lopez, P. Martins, S. Lanceros-Mendez, *Adv. Healthcare Mater.* **2018**, *7*, 1700845; c) L. Yang, X. Li, X. Ma, S. Xiong, P. Liu, Y. Tang, S. Cheng, Y.-Y. Hu, M. Liu, H. Chen, *J. Power Sources* **2018**, *381*, 171.

[10] Y. Hu, S. Mignani, J. P. Majoral, M. Shen, X. Shi, *Chem. Soc. Rev.* **2018**, *47*, 1874.

[11] A. Espinosa, R. Di Corato, J. Kolosnjaj-Tabi, P. Flaud, T. Pellegrino, C. Wilhelm, *ACS Nano* **2016**, *10*, 2436.

[12] M. V. Kovalenko, M. I. Bodnarchuk, R. T. Lechner, G. Hesser, F. Schäffler, W. Heiss, *J. Am. Chem. Soc.* **2007**, *129*, 6352.

[13] R. R. Shah, A. R. Dombrowsky, A. L. Paulson, M. P. Johnson, D. E. Nikles, C. S. Brazel, *Mater. Sci. Eng., C* **2016**, *68*, 18.

[14] a) X. Li, M. Tang, X. Feng, I. Hung, A. Rose, P.-H. Chien, Z. Gan, Y.-Y. Hu, *Chem. Mater.* **2017**, *29*, 8282; b) M. Unni, A. M. Uhl, S. Savliwala, B. H. Savitzky, R. Dhavalikar, N. Garraud, D. P. Arnold, L. F. Kourkoutis, J. S. Andrew, C. Rinaldi, *ACS Nano* **2017**, *11*, 2284.

[15] a) M. Frenkel, L. Dombrovsky, V. Multanen, V. Danchuk, I. Legchenkova, S. Shoval, Y. Bormashenko, B. P. Binks, E. Bormashenko, *J. Phys. Chem. B* **2018**, *122*, 7936. https://srd.nist.gov/JPCRD/jpcrdS2Vol11.pdf; b) E. Bormashenko, P. K. Roy, S. Shoval, I. Legchenkova, *Condens. Matter* **2020**, *5*, 62.

[16] D. Wang, L. Zhu, J.-F. Chen, L. Dai, *Angew. Chem., Int. Ed.* **2016**, *55*, 10795

[17] R. K. Vadivelu, H. Kamble, A. Munaz, N. T. Nguyen, *Sci. Rep.* **2017**, *7*, 12388.